

Synthesis of ZnS/ZnO Core-shell Nanostructures on Kevlar[®] Fiber

Jiun-Jr Wang², Wei-Chih Weng¹, Jo Lun Chiu¹, Yan Yu Chen¹, Chen Haw Su¹, Yu Sheng Tsai¹ and Hsiang Chen^{1,*}

¹Applied Materials and Optoelectronic Engineering, National Chi Nan University, Taiwan, ROC

²School of Medicine, Fu Jen Catholic University, New Taipei City, Taiwan, ROC

Received: January 6, 2018, Accepted: March 20, 2018, Available online: July 28, 2018

Abstract: ZnS/ZnO core-shell structures were synthesized on the Kevlar[®] fiber by the hydrothermal method. OD 600 antibacterial and material property tests revealed that 10 mins of ZnS sulfurization yielded optimal properties for ZnS/ZnO core-shell structures.

Keywords: Kevlar[®] fiber, ZnO, ZnS, antibacterial, core-shell structure

1. INTRODUCTION

Hexagonal wurtzite ZnO is an ideal semiconductor material [1,2,3], possessing electronic property of wide energy gap (3.37eV) [4]. Due to its photocatalytic [5,6], photoelectric, piezoelectric [7,8,9,10,11,12] and antimicrobial properties [13,14,15,16], ZnO has been regarded as a superior material for sensor construction against other materials. ZnS is another semiconductor material with low toxicity and wide energy gap (3.6~3.8eV) [17], and has formerly been used as optical sensor material. ZnS was commonly synthesized in combination with other materials, notably ZnO [23]. ZnS/ZnO core-shell has been used in various photoelectric [24,25,26] and biological sensors [27]. Several methods were developed for growing ZnO nanostructures, while hydrothermal technique has been regarded as an efficient and cost-effective method, since ZnO nanorods can grow at relatively low temperature (below 100 degrees Celsius) in a short period of time [28,29,30,31,32,33]. In this study, we used hydrothermal technique to grow ZnO nanorods on the Kevlar[®] fiber, followed by ZnS shell on ZnO nanorods. We then examined associations between changes in surface morphology and material properties of ZnS/ZnO core-shell structure and ZnS sulfurization time.

In addition, ZnS/ZnO core-shell structure possesses antimicrobial capacity, a critical property of invasive sensor. Kevlar[®] fiber, a para-aramid synthetic fiber, is a high-strength light-weight material, well-known for its role in flexible armor manufacture [34,35,36,37,38,39]. ZnO nanorods (NRs) grown Kevlar[®] fiber

[40,41,42] has been used as a flexible piezoelectric material [44] and in flexible fiber-optic sensor synthesis [43]. However, the technique to grow ZnS/ZnO core-shell structure on Kevlar[®] fiber has never been reported. In this study, we developed a method to grow ZnS/ZnO core-shell structure on Kevlar[®] fiber and examined its material properties. We expect this study will improve synthesis of soft substrates and flexible fiber optic sensor.

Material properties of ZnS/ZnO core-shell structure were examined in 5 aspects: (1) the size and surface morphology of single Kevlar[®] fiber were examined via optical microscope (OM). (2) Surface structures of ZnS/ZnO core-shell grown on the Kevlar[®] fiber were assessed via large ratio field emission scanning electron microscope (FESEM). (3) Crystal chemical analysis of material properties and the chemical bindings of element composition were examined via Energy Dispersive X-Ray Spectrometer (EDS) analysis, X-ray diffraction (XRD) and High-resolution X-ray Photoelectron Spectrometer (XPS), respectively. (4) Antibacterial capacity of ZnS/ZnO core-shell was evaluated via the OD 600 antibacterial test.

2. EXPERIMENT

A 2x2 square centimeters Kevlar[®] fiber was thoroughly washed with acetone and ethanol to remove organic pollutants, then waxed together with a 2x2 square centimeters silicon substrate. ZnO seed layer was prepared by a spin-coating liquid, made by 0.66 g of zinc acetate and 2 drops of ethanolamine (MEA) in 60 ml ethanol, heated via heated circulating bath for 30 min at 60 °C, followed by immersing in clarifying fluid for 24 hours. ZnO seed layer was

*To whom correspondence should be addressed: Email: hchen@ncnu.edu.tw
Phone: +886 492910960; fax: +886 492912238

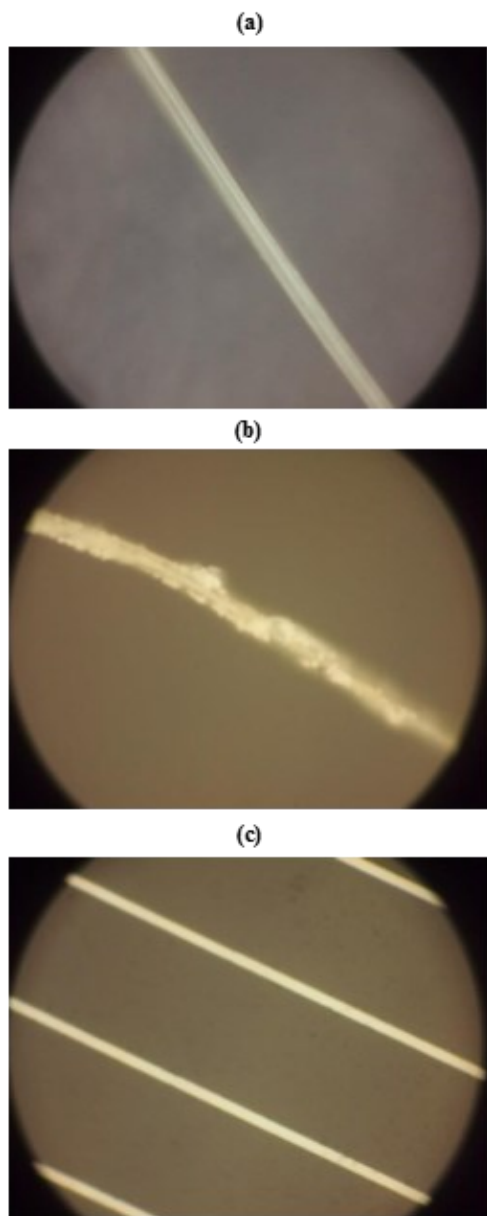


Figure 1. Optical microscopic images of a Kevlar[®] fiber (a) and a Kevlar[®] fiber with ZnS/ZnO core-shell nanostructures. The scale of 100 μm between grids was shown in (c). Images were in the same magnification.

planted on the Kevlar[®] fiber layer through a spin coating procedure, by which 3 to 5 droplets of ZnO seeds were dripped on Kevlar[®] fiber; after 30 s of spin coating, ZnO-coated Kevlar[®] fiber was heated at 70 $^{\circ}\text{C}$ for 5 min. The spin coating procedure was repeated five times.

After removing wax, ZnO-coated Kevlar[®] fiber was placed in a solution, containing 0.9468g of zinc nitrate and 0.98126g of hexamethylenetetramine, heated at 80 $^{\circ}\text{C}$ for 60 min to grow ZnO nanorods, which in turn were immersed in a solution, containing 2.4018g of sodium sulfide nonahydrate, heated at 70 $^{\circ}\text{C}$ to grow ZnS shells at 0, 5, 10, 15 and 20 min.

3. RESULTS AND DISCUSSION

Fig. 1 shows optical microscopic images of a Kevlar[®] fiber (a) and a Kevlar[®] fiber with ZnS/ZnO core-shell nanostructures (b) and a scale of 100 μm shown between grids (c); images were taken at the same magnification rate of 400. The diameter of a Kevlar[®] fiber was estimated at around 15 μm , with respect to the scale of Fig. 1(c), and with ZnS/ZnO core-shell nanostructures grown on Kevlar[®] fiber, its diameter increased by around 10%.

Fig. 2 shows FESEM images of surface morphology of ZnS/ZnO core-shell nanostructures grown on the Kevlar[®] fiber, at 5 min (X10K) (a), 5 min (X50K) (b), 15 min (c) and 20 min (d) of ZnS sulfurization time. Results showed that ZnS/ZnO core-shell nanostructures was observable on the Kevlar[®] fiber following 5 min of ZnS sulfurization. With the increase of time, the surface of the ZnO nanorods was rough at 5 min of sulfurization (Fig. 2(b)), then became smooth at 10 min of sulfurization and onwards, whereas the nanorods shrunk in size after 10 minutes (Fig. 2(c) and (d)).

The surface of ZnO nanorods became smoother at 10 min of sulfurization and onward (Fig. 2(c) and (d)).

Fig. 3 shows EDS analysis of ZnS/ZnO core-shell nanostructures synthesized at 5 min (a), 10 min (b), 15 min (c) and 20 min (d) ZnS of sulfurization time. Sulfur elements were detected as early as 5 min of sulfurization, supporting that ZnS shell was successfully attached to the ZnO nanorods (NRs); the rough surface shown on Fig. 2 (b) was attributed to small amount of ZnS crystals attached to the surface. The smooth surface of ZnO nanorods observed at Fig. 2(c) and (d) was likely attributed to the saturation of ZnS sulfurization. On the other hand, ZnS sulfurization beyond 10 min would cause disintegration of ZnS responding to S^{2-} causing smaller nanotubes.

Chemical equations describing the ZnS and ZnO interaction are shown below.

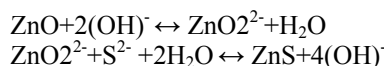


Fig. 4 shows X-ray diffraction analysis of crystal lattice of ZnS/ZnO core-shell structures on Kevlar[®] fiber. XRD peaks for Kevlar[®] fiber at 5 min and 10 min of sulfurization were 20.56 and 22.84, respectively. The crystal structures of the Kevlar[®] fiber were shown at lattice (110) and (200) [40, 45]. Peaks of (100), (002), (101) and (102), (110), (103), (112) on the ZnS/ZnO 20 min curve was the evidence that ZnO nanorods were successfully grown on the Kevlar[®] fiber. Note that ZnS shell structure was shown on a high peak (111). Due to the ZnS accumulation as described above, we can infer that ZnS would increase and became higher than ZnO gradually. the peak of ZnS is higher than the peak of ZnO.

Fig. 5 shows chemical analysis of ZnS/ZnO core-shell structures by means of XPS. Chemical elements of Kevlar[®] fiber were C 1s and N 1s, while chemical elements of ZnS/ZnO core-shell structures were Zn 2p, O 1s, and S 2p's peak.

Finally, the OD 600 antibacterial test was adopted to examine the antimicrobial capacity of ZnS/ZnO core-shell structures. OD600 is the abbreviation of optical density for light at 600 nm. The instrument detected the light absorbance value of Escherichia coli (E.

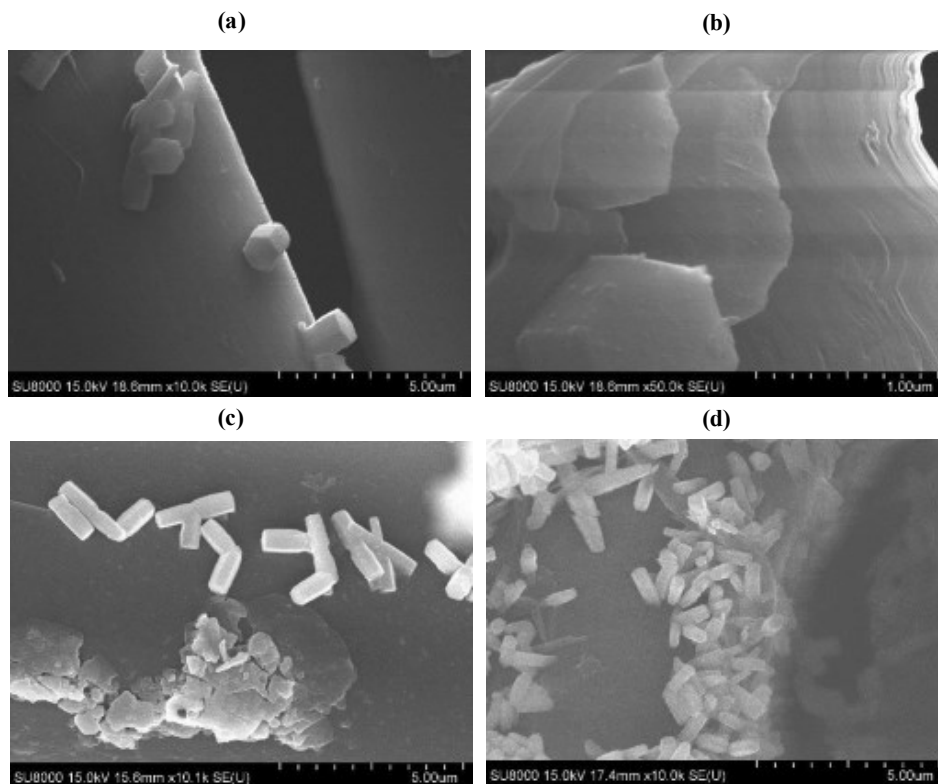


Figure 2. FESEM images of the ZnS/ZnO core-shell nanostructures synthesized at (a) 5 min (X10K) (b) 5 min (X50K) (c) 15 min (X10K) and (d) 20 min (X10K) of ZnS sulfurization time.

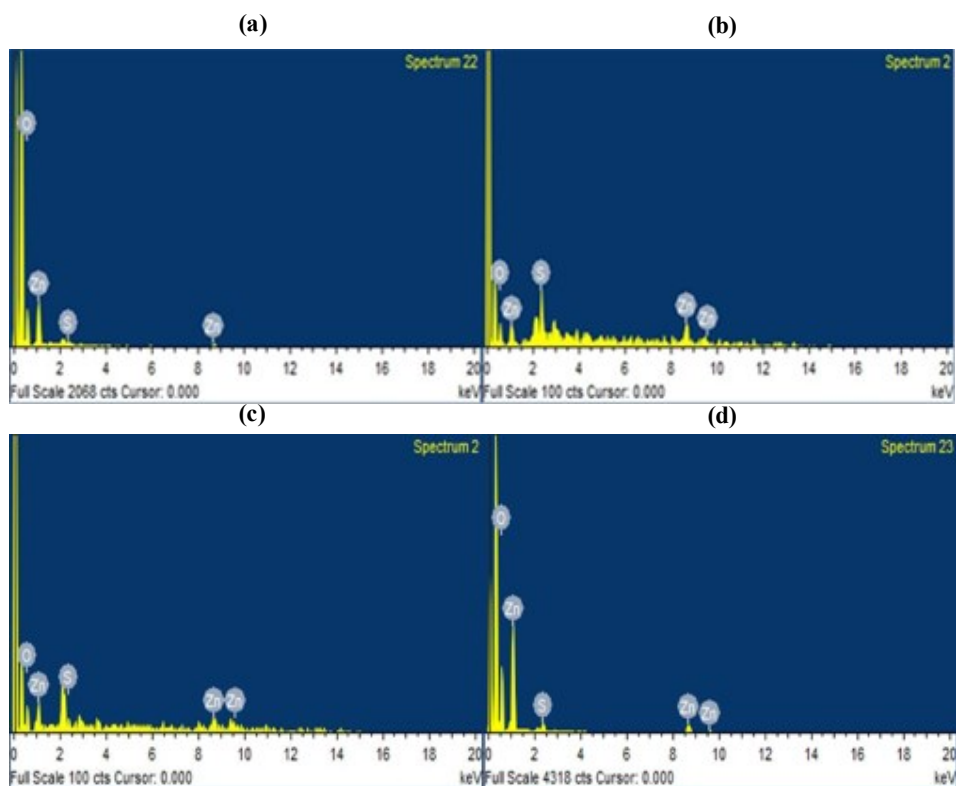


Figure 3. EDS analysis of the ZnS/ZnO core-shell nanostructures at 5 min (a), 10 min (b), 15 min (c) and 20 min (d) of ZnS sulfurization time

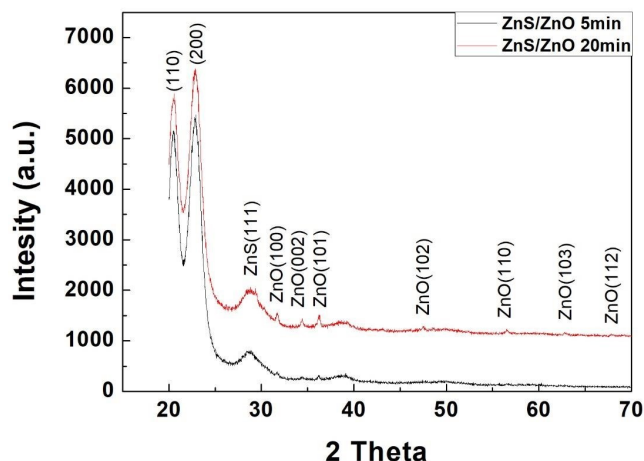


Figure 4. XRD pattern of the ZnS/ZnO core-shell structures at 5 min and 20 min of sulfurization time

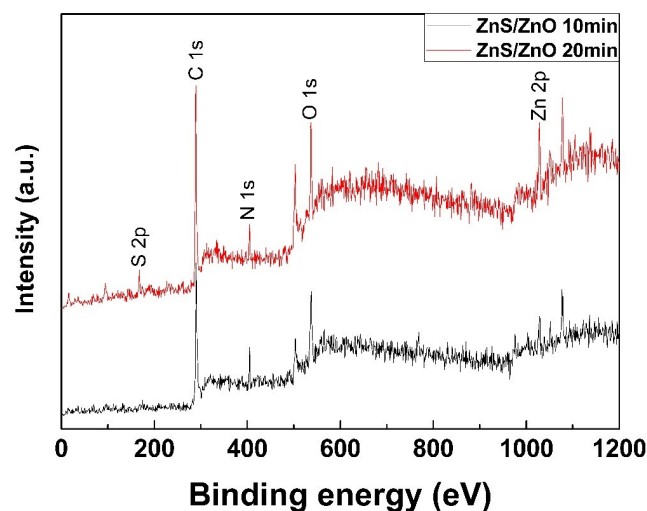


Figure 5. The wide scan XPS spectra of the ZnS/ZnO core-shell nanostructures with at 10 min and 20 min of sulfurization time

coli) solution at 600nm wavelength. The absorbance value is proportional to the concentration of *E. coli* in solution. It can calculate the bacterial growth rate of this material. The Kevlar® fibers with ZnS/ZnO core-shell synthesized at 0, 10, 15 and 20 min of sulfurization were immersed in *Escherichia coli* cells suspended in aqueous solution. *Escherichia coli* populations, measured via photoelectric colorimeter at a wavelength of 600 nm at various timeline, were compared with the same *Escherichia coli* solution without ZnS/ZnO nanostructures. Fig. 6 demonstrated that ZnS/ZnO core-shell structures synthesized at 10 min of sulfurization exhibited significant resistance to *Escherichia coli* growth; its antimicrobial capacity decreased when ZnO sulfurization was longer than 10 min. According to the formula $ZnO_2^{2-} + S^{2-} + 2H_2O \rightarrow ZnS + 4(OH)^-$, when the reaction lasted more than 10 minutes, the material constitution gradually reacted back to S^{2-} , which antibacterial effect will become worse because the saturation of ZnS. ZnO and ZnS both

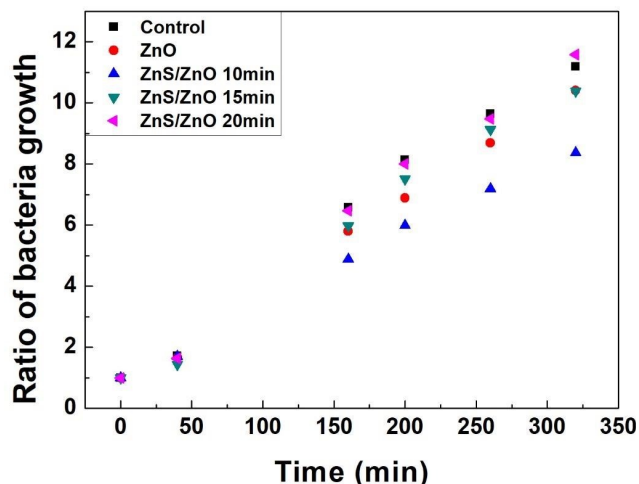


Figure 6. Ratio of bacteria growth on the ZnS/ZnO core-shell structures at 0, 10, 15, and 20 min of sulfurization, examined via OD 600 Test.

have antibacterial effect. 20 minutes group is worse than the control group, which within the experimental offset range. 10 minutes group had best antibacterial effect among all the samples. The result was consistent with the findings by FESEM analysis.

4. CONCLUSIONS

We successfully developed a technique to grow ZnS/ZnO core-shell structures on the Kevlar® fiber. By examining its material properties, ZnS/ZnO core-shell structures exhibited excellent ZnS shell with optimal antibacterial capacity at 10 min of sulfurization. In this study, we provided a feasible soft substrate for ZnS/ZnO core-shell structures synthesized on the Kevlar® fiber and a candidate material for future construction of fiber-optic sensors.

REFERENCES

- [1] F. Fleischhaker, V. Wloka and I. Hennig, *Journal of Materials Chemistry*, 20, 6622 (2010).
- [2] P. Struk, T. Pustelny and Z. Opilski, *Acta Physica Polonica-Series A General Physics*, 118, 1239 (2010).
- [3] C.-Y. Tsay, K.-S. Fan, S.-H. Chen and C.-H. Tsai, *Journal of Alloys and Compounds*, 495, 126 (2010).
- [4] A. McLaren, T. Valdes-Solis, G. Li and S. C. Tsang, *Journal of the American Chemical Society*, 131, 12540 (2009).
- [5] X. Zhang, J. Qin, Y. Xue, P. Yu, B. Zhang, L. Wang and R. Liu, *Scientific reports*, 4 (2014).
- [6] M. El-Kemary, H. El-Shamy and I. El-Mehasseb, *Journal of Luminescence*, 130, 2327 (2010).
- [7] F. L. Tzec, M. A. Frutis, G. R. Gattorno and G. Oskam, *Journal of New Materials for Electrochemical Systems*, 16, 209 (2013).
- [8] A. K. Zak, M. E. Abrishami, W. A. Majid, R. Yousefi and S. Hosseini, *Ceramics International*, 37, 393 (2011).
- [9] M. Rahman, A. Umar, L. Roza, S. Samsuri, M. Salleh, I. Iwan-tono and T. Tugirin, *Journal of New Materials for Electrochem-*

- ical Systems, 18, 213 (2015).
- [10] L. Xu, X. Li, Y. Chen and F. Xu, *Applied Surface Science*, 257, 4031 (2011).
- [11] Q. Yang, W. Wang, S. Xu and Z. L. Wang, *Nano letters*, 11, 4012 (2011).
- [12] B. Kumar and S.-W. Kim, *Nano Energy*, 1, 342 (2012).
- [13] N. Talebian, S. M. Amininezhad and M. Douidi, *Journal of Photochemistry and Photobiology B: Biology*, 120, 66 (2013).
- [14] Y.-C. Shyu, T. S. Chieh, W. M. Su, C.-C. Lu, C.-Y. Weng, L. Y. Shan, H. C. Hao, J.-J. Lin, C. F. Lin and C.-T. R. Yu, *Journal of New Materials for Electrochemical Systems*, 19, 229 (2017).
- [15] K. R. Raghupathi, R. T. Koodali and A. C. Manna, *Langmuir*, 27, 4020 (2011).
- [16] Y. Xie, Y. He, P. L. Irwin, T. Jin and X. Shi, *Applied and environmental microbiology*, 77, 2325 (2011).
- [17] K. Tiwary, S. K. Choubey and K. Sharma, *Chalcogenide Letters*, 10, 319 (2013).
- [18] F. Haque, K. Rahman, M. Islam, M. Rashid, M. Akhtaruzza-man, M. Alam, Z. Alothman, K. Sopian and N. Amin, *Chalcogenide Letters*, 11, 189 (2014).
- [19] D. H. Hwang, J. H. Ahn, K. N. Hui, K. San Hui and Y. G. Son, *Nanoscale research letters*, 7, 26 (2012).
- [20] A. GADALLA, M. A. EL-SADEK and R. HAMOOD, *Chalcogenide Letters*, 14 (2017).
- [21] N. Soltani, E. Saion, M. Erfani, A. Bahrami, M. Navaseri, K. Rezaee and M. Z. Hussein, *Chalcogenide Letters*, 9 (2012).
- [22] T. Serrano, J. Cavazos, Y. Peña and I. Gómez, *Chalcogenide Letters*, 11, 21 (2014).
- [23] T. YU, K. WANG, Y. CHEN, M. SHEU and H. CHEN, *Chalcogenide Letters*, 14 (2017).
- [24] H. X. Sang, X. T. Wang, C. C. Fan and F. Wang, *international journal of hydrogen energy*, 37, 1348 (2012).
- [25] K. Wang, J. Chen, Z. Zeng, J. Tarr, W. Zhou, Y. Zhang, Y. Yan, C. Jiang, J. Pern and A. Mascarenhas, *Applied Physics Letters*, 96, 123105 (2010).
- [26] S. Tarish, Z. Wang, A. Al-Haddad, C. Wang, A. Ispas, H. Romanus, P. Schaaf and Y. Lei, *The Journal of Physical Chemistry C*, 119, 1575 (2015).
- [27] Y.-M. Sung, K. Noh, W.-C. Kwak and T. G. Kim, *Sensors and Actuators B: Chemical*, 161, 453 (2012).
- [28] S. Baruah and J. Dutta, *Science and Technology of Advanced Materials*, 10, 013001 (2009).
- [29] T.-Y. Yu, Y. C. Chen, W. T. Chiu, Y. Luo, S. S. Wang, H. Chen, H. Y. Shin, M. H. Lin, K. Y. Wang and Y. Y. He, *Journal of New Materials for Electrochemical Systems*, 19, 181 (2016).
- [30] J. Xie, H. Wang, M. Duan and L. Zhang, *Applied surface science*, 257, 6358 (2011).
- [31] S. H. Ko, D. Lee, H. W. Kang, K. H. Nam, J. Y. Yeo, S. J. Hong, C. P. Grigoropoulos and H. J. Sung, *Nano letters*, 11, 666 (2011).
- [32] Y. Tao, M. Fu, A. Zhao, D. He and Y. Wang, *Journal of Alloys and compounds*, 489, 99 (2010).
- [33] H. Chen, W. M. Su, Y.-T. Chen, C.-C. Lu and C.-Y. Weng, *Journal of New Materials for Electrochemical Systems*, 20, 049 (2017).
- [34] M. Su, A. Gu, G. Liang and L. Yuan, *Applied Surface Science*, 257, 3158 (2011).
- [35] Y. Park, Y. Kim, A. H. Baluch and C.-G. Kim, *International Journal of Impact Engineering*, 72, 67 (2014).
- [36] J. Lim, J. Q. Zheng, K. Masters and W. W. Chen, *International Journal of Impact Engineering*, 38, 219 (2011).
- [37] T.-T. Li, R. Wang, C.-W. Lou and J.-H. Lin, *Composites Part B: Engineering*, 59, 60 (2014).
- [38] J. Lim, W. W. Chen and J. Q. Zheng, *Polymer Testing*, 29, 701 (2010).
- [39] A. Majumdar, B. S. Butola and A. Srivastava, *Materials & Design*, 51, 148 (2013).
- [40] A. Hazarika, B. K. Deka, D. Kim, K. Kong, Y.-B. Park and H. W. Park, *Composites Part A: Applied Science and Manufacturing*, 78, 284 (2015).
- [41] H.-S. Hwang, M. H. Malakooti, B. A. Patterson and H. A. Sodano, *Composites Science and Technology*, 107, 75 (2015).
- [42] H.-S. Hwang, M. H. Malakooti and H. A. Sodano, *Composites Part A: Applied Science and Manufacturing*, 76, 326 (2015).
- [43] J. Liu, W. Wu, S. Bai and Y. Qin, *ACS applied materials & interfaces*, 3, 4197 (2011).
- [44] M. H. Malakooti, B. A. Patterson, H.-S. Hwang and H. A. Sodano, *Energy & Environmental Science*, 9, 634 (2016).
- [45] H. Kong, C. Teng, X. Liu, J. Zhou, H. Zhong, Y. Zhang, K. Han and M. Yu, *RSC Advances*, 4, 20599 (2014).

